Macromolecules

Article

pubs.acs.org/Macromolecules

Dynamic Changes in Structural Color of a Lamellar Block Copolymer Photonic Gel during Solvent Evaporation

Wonmok Lee,[†,⊥] Jongseung Yoon,[‡,⊥] Edwin L. Thomas,[*,§] and Hyunjung Lee[*,∥]

[†]Department of Chemistry, Sejong University, 98 Gunja-dong, Gwangjin-gu, Seoul, Korea 143-747

[‡]Department of Chemical Engineering and Materials Science, University of Southern California, Los Angeles, California 90089, United States

[§]Department of Mechanical Engineering and Materials Science, Rice University, Houston, Texas 77030, United States

[∥]School of Advanced Materials Engineering, Kookmin University, Jeongneung-ro 77, Seoul, Korea 136-702

ABSTRACT: A high molecular weight, lamellar block copolymer (BCP) can exhibit a photonic stop band in the visible range of wavelengths due to the one-dimensional periodic dielectric layer structure. After dissolving a high molecular weight BCP in a neutral solvent, solvent evaporation causes microphase separation, forming a so-called "photonic gel" at a quite low polymer concentration (~10 wt %). Moreover, by allowing the solvent to further evaporate, the reflected color can be tuned over the entire range of the visible spectrum. Here, a polystyrene−polyisoprene diblock (PS-*b*-PI) is dissolved in cumene, and the solution was placed between two glass substrates. The radial concentration gradient during slow evaporation of the cumene generates a "rainbow-like" set of reflected colors from the photonic gel. Based on local measurement of the reflectivity along the radial direction of the photonic gel, the radial solvent composition was calculated and the experimentally observed reflectivity was compared to results simulated using the transfer matrix method. Balsara's scaling law for the lamellar period versus polymer concentration was adapted for the simulation of the concentration profile, which showed a reasonable agreement with a previous theoretical calculation. Compared to the simulated spectra, experimentally obtained reflectance spectra exhibited weaker peak reflectivity and additional peak broadening due to lamellar misorientation and decrease of the average grain size during solvent evaporation.

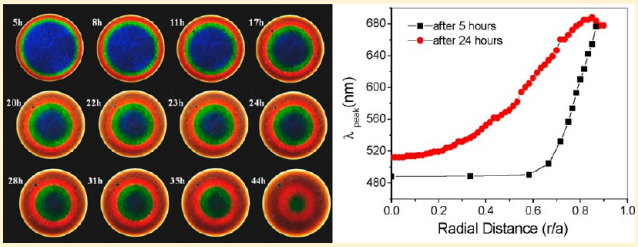

INTRODUCTION

Self-assembled structures of block copolymers (BCP) tailored by block size, composition, and persistent length have drawn much attention as materials building block for various nanotechnologies.[1,2] Many applications have been developed, and the microphase separation mechanism of BCP from the thermodynamic point of view has been studied for optimizing the properties.[3−5] One of the exciting applications of BCPs is the so-called photonic crystal.[6−9] A photonic crystal enables manipulation of light such as confinement, amplification, beam steering, etc., in the visible and near-infrared (NIR) regimes. A visible range photonic crystal is comprised of a periodic dielectric structure with a unit lattice size on the submicrometer scale. This requires a total BCP molecular weight as large as half million g/mol for a solvent-free sample. Recently, various photonic crystal structures from high molecular weight BCPs have been introduced, and successful applications of BCP photonic crystal for laser mirrors[10] and thermochromic and mechanical pressure sensors have been reported.[11−15] Theoretically, the segregation strength of a BCP depends on the degree of polymerization (N) and the Flory−Huggins interaction parameter (χ).[13] For a BCP solution diluted by a solvent neutral to each block, χ decreases compared to the bulk sample. Because of their high molecular weights (i.e., large N), photonic BCPs can microphase separate at very low polymer concentration. Thus, as solvent evaporates, microphase separation takes place above a threshold concentration (i.e., the order−disorder transition concentration) at a constant temperature.

We recently reported that a nearly symmetric composition, high molecular weight PS-*b*-PI exhibits a well-ordered lamellar morphology even at a concentration as low as ~10 wt % in nonselective solvent (i.e., cumene).[11,12,16] Because of a large lamellar spacing (~200 nm) which reflects light of wavelengths in the visible regime, an intriguing thermochromic behavior due to the temperature dependence of the Flory−Huggins interaction parameter of the BCP photonic gel could be visually monitored. The lamellar period of the BCP microstructure in solution exhibits scaling behavior with respect to the concentration,[17] which was confirmed experimentally using SAXS. However, visualization of the detailed domain microstructure of a dilute but microphase-separated BCP solution is difficult. In the present report, we focus our attention to the isothermal changes of domain refractive index and reflective color of a BCP photonic gel originating from variations in the lamellar domain spacing due to radial mass transport of solvent

Received: December 12, 2012
Revised: March 17, 2013
Published: August 6, 2013

   dx.doi.org/10.1021/ma302557v | *Macromolecules* 2013, 46, 6528−6532

and the subsequent polymer concentration gradient with solvent evaporation at the radial edge. In addition to the colorimetric and spectroscopic analyses, laser scanning confocal microscopy (LSCM) is utilized to elucidate the detailed grain structure of the BCP photonic gel on a real time basis (1 s/image).

EXPERIMENTAL SECTION

Materials. The high molecular weight BCP system used in this study was PS(480K)-*b*-PI(360K) anionically polymerized in a glovebox using benzene/cyclohexane mixed solvent. The detailed procedure for the synthesis is described in our earlier publication.[16] Cumene (99%, Aldrich) was used without further purification.

Sample Casting. The BCP was dissolved in cumene (10%, w/w) for several days. The solution exhibited a greenish-blue color due to the selective reflection of visible light from the self-assembled lamellar BCP gel. As shown in Figure 1, a drop of the BCP gel was confined between two cover glasses to form a 10−100 μm thick layer. The solvent was then allowed to evaporate continuously over approximately 2 days. The initially transparent-blue film developed a set of intensely colored concentric rings in 1−2 h, and these color rings moved radially inward with time. A series of pictures were taken over the course of almost 2 days at several hour intervals as shown in Figure 1.

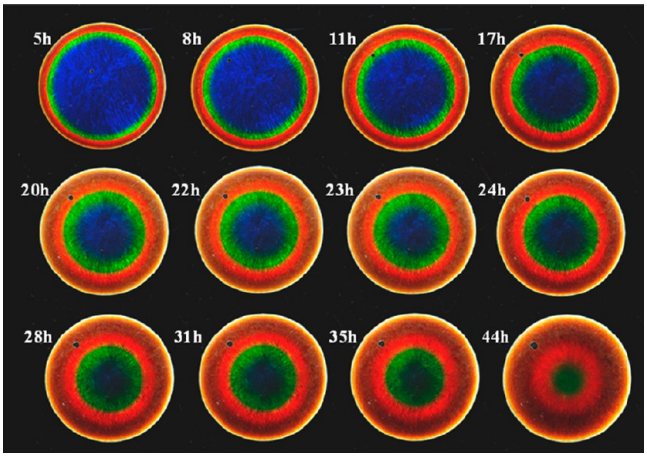

Figure 1. Time series images of a "rainbow" of colors of the PS-*b*-PI BCP photonic gel showing the movement of the continuous concentric color rings covering the entire range of visible wavelengths. The first picture was taken 5 h after casting, and the following pictures were taken at the times indicated. Evaporation of cumene from the outer rim of the specimen raises the χ parameter and induces a net extension of the chain dimensions along the lamellar normal, despite the contraction of the layers due to loss of solvent, resulting in an overall red-shift.

Reflectivity Measurements. The optical response of a 12.7 mm diameter and 40 μm thick sample was investigated by taking reflectivity measurements using a Zeiss Axioscope equipped with a fiber-optic spectrometer (Stellarnet EPP2000)[16] (Figure 1). A silver-coated metallic mirror was used as a 100% reference. In order to get the reflectivity at specific radial location, the smallest aperture (~0.5 mm) size of objective lens (10×, Leica, numerical aperture (NA) = 0.3) was employed.

LSCM Imaging. In-situ optical images of the photonic gel film during drying were obtained using a laser scanning confocal microscope (LSCM, Leica, TCS). The reflection mode of LSCM was used in which reflection signals of the probe light λ = 488 nm) were scanned through an oil-immersion objective lens (Leica, HCX PL APO 63×, N.A.= 1.4). Each image was acquired in about 1 s.

SEM and TEM Analysis. The photonic gel was slowly cast from cumene between two cover glasses until the solvent entirely dries out. The 50 μm thick dry film was freeze-fractured under liquid nitrogen, and the cross section was imaged by using scanning electron microscopy (SEM, JEOL JSM-6701F). A thicker film (~1 mm thick) using the same PS-*b*-PI was slowly cast and microtomed to obtain thin (~100 nm) slice of the dry BCP film. After being stained with OsO_4 for 1 h, the specimen was imaged in bright field transmission electron microscopy (TEM, JEOL-200CX).

RESULTS AND DISCUSSION

Structural Color Changes of Block Copolymer Gel. In our previous study,[11] thermochromic behavior of the confined PS-*b*-PI photonic gel at a constant polymer concentration was interpreted in terms of both the change of refractive indices and domain thicknesses with temperature, where the latter effect was dominant due to the variation of temperature-dependent segregation strength (i.e., χT)) between PS and PI blocks. The segregation power between blocks in photonic gels can be also controlled by varying the solvent concentration at constant temperature. Here, we describe the effect of solvent concentration change on morphologies and the spectral properties of PS-*b*-PI photonic gels confined between glass substrates.

We first prepared a 10.5 wt % of solution of the PS-*b*-PI BCP in cumene, which is a nonselective, good solvent to both PS and PI.[11] After casting, solvent evaporation causes microphase separation and the film becomes gel-like with a green-blue reflective color. The color became more intense when the solution was cast between two glass substrates (BCP film thickness ~40 μm) due to the confinement-induced orientation of the lamellar domains. The temperature was maintained at room temperature while the solvent evaporated outward at the rim of the confining glass super/substrates which resulted in a gradient of solvent concentration along the radial direction. The sample gradually developed reflective colors covering almost the entire range of visible wavelengths as a function of sample position (i.e., from the edge (red-brown) to the center (blue). Figure 1 presents a time lapse series of photographic images of a confined BCP gel taken at different times of solvent evaporation. The reflective color appeared blue in most areas of the sample after 5 h of solvent evaporation. Annular areas of green to red colors were observed to slowly move toward the center, with the intensity of blue color at the central region becoming weaker.

After the BCP solution was completely dried between two glass substrates over several weeks, the sample was freeze-fractured and the cross-sectional morphology was observed by SEM. As shown in Figure 2a,c, grains of lamellar domains were found at various angles but more or less oriented parallel to the two glass substrates. The observed lamellar domain spacing in the SEM images in Figure 2c matched well with that of a bulk sample (Figure 2d).

Reflectance spectra for near-normal incidence were measured at various spots along the radial direction at various times of solvent evaporation. As is evident from Figure 3a, there is a continuous red-shift in the wavelength of the reflectance maxima with times of solvent evaporation. The reflectance peak at the central region is at 490 nm with a full width at half-maximum (fwhm) of 11 nm for a polymer concentration of 0.105. The continuous change of the peak reflectivity wavelength along the radial direction is presented in Figure 4 by plotting λ_{peak} as a function of radial positions at 5 and 24 h of solvent evaporation. Figure 3a shows data after 5 h of solvent

dx.doi.org/10.1021/ma302557v | *Macromolecules* 2013, 46, 6528−6532

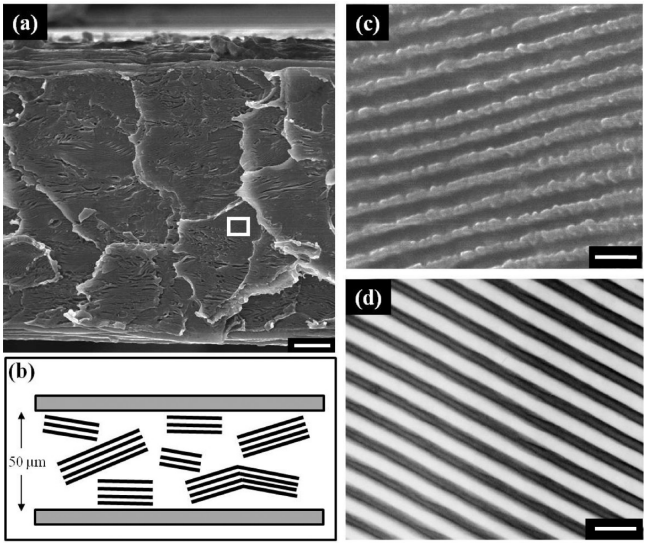

Figure 2. Cross-sectional SEM (a, c) and TEM (d) images of the photonic PS-*b*-PI film cast between two glass coverslips. As shown in (a), various grains of lamellae are evident. (b) Schematic diagram of grain orientations. (c) Enlarged SEM image of the region indicated by the small white box in (a). The glassy PS layers are the thicker and smoother features, while the PI layers are rougher and thinner. (d) TEM image of dry PS-*b*-PI film after staining with OsO_4. Dark regions correspond to OsO_4 stained PI layers. The dry film has a period of 200 nm with 110 nm thick PS layers and 90 nm thick PI layers as evident in both the SEM and TEM images. The scale bar shown in (a) is 5 μm, and those in (c, d) are 300 nm.

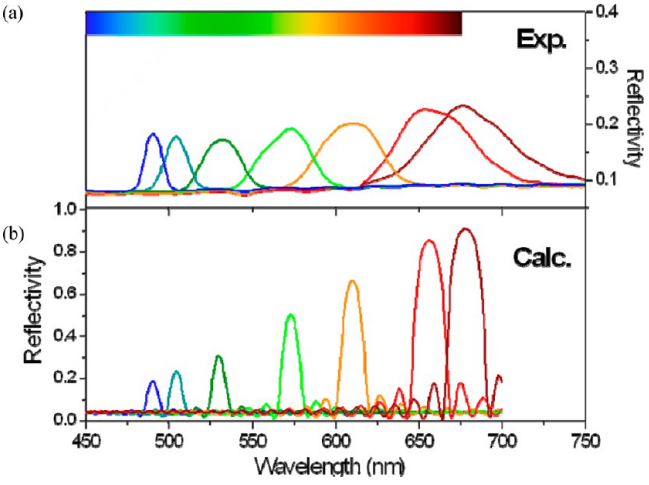

Figure 3. (a) Reflectivity spectra of the BCP photonic gel at various radial positions measured after 5 h of solvent evaporation. (b) Transfer matrix method calculation of the simulated reflectivities of lamellar BCPs using the different indices of refraction and thicknesses of unit layers of each block as listed in Table 1. Significant reflectivity peak broadening is observed as the sample dries.

evaporation. The wavelength of the peak reflection (λ_{peak}) red-shifted from approximately 490 nm in the center to about 680 nm near the rim, with an increase in reflectance from 20% to 25% as well as with a significant peak broadening from fwhm = 13 nm to fwhm = 57 nm as illustrated in Figure 3a and Table 1.

Modeling of Reflectivity: Transfer Matrix Method. Having measured the reflectivity spectra, we can construct a simple mathematical model to describe the dynamic changes of reflective colors in confined BCP gels during slow solvent

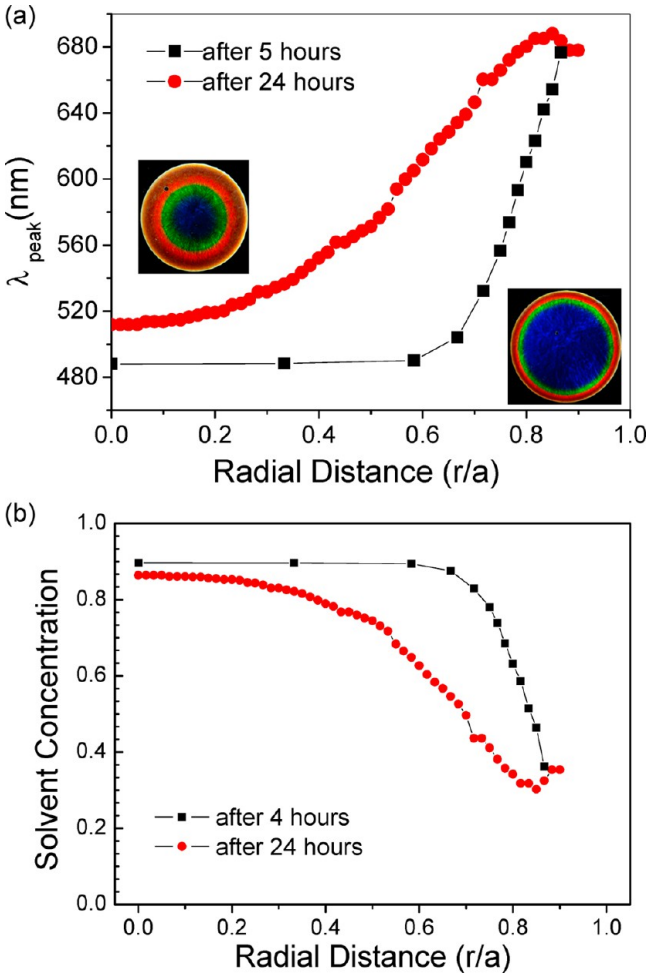

Figure 4. (a) Plot of λ_{peak} vs radial distance taken after 5 and 24 h of solvent evaporation. Continuity of λ_{peak} along the radial direction is clearly shown for both plots, even though the human eye sees distinct color rings. (b) Plot of the calculated solvent concentration vs radial distance. Solvent concentration was calculated according to the relationship of λ_{peak} and ϕ_p based on eqs 2 and 3.

Table 1. Calculated Material Parameters for Input to TMM for the Reflectivity Simulations in Figure 3b

λ_{peak} (nm)	ϕ_p (w/w)	n_H	n_L	L (nm)	t_H (nm)	t_L (nm)
490	0.105	1.501	1.493	163.6	90.0	73.6
504	0.125	1.503	1.493	168.2	92.5	75.7
530	0.166	1.507	1.494	176.4	97.0	79.4
573	0.260	1.517	1.496	190.1	104.5	85.5
610	0.368	1.527	1.498	201.4	110.8	90.6
656	0.544	1.545	1.501	215.0	118.3	96.8
678	0.647	1.555	1.503	221.3	121.7	99.6

evaporation. For the calculation of the reflectivity spectra of a finite 1D periodic structure, the transfer matrix method[11,18] (TMM) was used with several assumptions. First, we assume that cumene solvates the PS and the PI layers nonselectively. Therefore, the microstructure of the BCP gels retains the lamellar morphology throughout the entire concentration range. Second, we assume the orientation of the lamellae to be perfectly parallel to the glass substrate. With this assumption, we can model the visible spectra as arising from normal reflection of light at the lamellar interfaces. Third, we assume the number of lamellar periods (M) is fixed at 200. M is

dx.doi.org/10.1021/ma302557v | *Macromolecules* 2013, 46, 6528–6532

estimated considering the thickness of fully dried film between glass substrates and the lamellar spacing L observed in TEM (hence $M = t/L$). Fourth, we assume the lamellar domain periodicity L follows the relationship with volume fraction of polymer ϕ given by $L \propto (\phi_p)^{1/6}$ as suggested by Balsara and co-workers.[17] They showed that the thermodynamically controlled lamellar domain periodicity in a nonselective solvent satisfies this scaling dependence at strong segregation regime. Using Bragg's law and the Balsara's relationship, the peak wavelength of reflected light from multilayer stacks of low refractive index contrast can be expressed as eq 1, where λ_{peak} is the first-order peak wavelength at normal incidence, n_{eff} is the solvent-dependent average index of refraction of the dielectric stack, and α is a proportionality constant.

$$\lambda_{peak} = 2n_{eff}(\phi_p)L(\phi_p) \cong 2\alpha n_{eff}(\phi_p)\phi_p^{1/6} \quad (1)$$

Employing the experimentally measured λ_{peak} and assuming the polymer concentration at the center of the sample after 5 h of solvent evaporation to be the same as the as initially prepared polymer concentration in cumene ($\phi_p = 0.105$), we were able to calculate the proportionality constant $2\alpha = 476$ nm.

The effective domain refractive index at a given concentration can be estimated using the bulk refractive index of each polymer ($n_{PS} = 1.590$, $n_{PI} = 1.510$) and that of cumene ($n_{cumene} = 1.491$). Adopting the rule of mixtures as used in our previous report,[4,11] we can estimate n_H and n_L which are refractive indices of solvated PS and PI layers, respectively:

$$n_H = \phi_p n_{PS} + (1 - \phi_p)n_{cumene} \quad (2)$$

$$n_L = \phi_p n_{PI} + (1 - \phi_p)n_{cumene} \quad (3)$$

Because of the small difference between n_{PI} and n_{cumene}, n_L remains nearly constant with solvent concentrations. Assuming that the dry film layer thickness ratio of the PS domain to PI domain in bulk (as determined from TEM) is maintained in all of the swollen states (i.e., a nonselective solvent), we have $t_H/t_L = 11/9$. This yields a n_{eff} of lamellar photonic gel as

$$n_{eff} = 0.55n_H + 0.45n_L \quad (4)$$

In eq 1, $n_{eff}(\phi_p)$ is determined by combining eqs 2, 3, and 4. The polymer volume fraction which corresponds to each experimental reflection maxima could be then calculated, followed by calculation of n_H, n_L, and n_{eff} using eqs 2–4. The calculated results are listed in Table 1. These parameters were then used as the input values for TMM calculations which are shown as the series of spectra in Figure 3b. As shown in Figure 3a,b, combining the effects of both the polymer composition dependence of the lamellar domain spacings and the polymer composition dependence of the respective refractive indices predicts a systematic red-shift but with a stronger increases in peak intensity and a significantly narrower peak width.

Equation 1 also enables the estimation of polymer concentration vs relative radial distance at various times during evaporation using the data shown in Figure 4a, where r is radial position and a is the radius of glass substrate ($a = 6.35$ mm). Figure 4b represents the behavior of solvent composition calculated from λ_{peak} data as a function of relative radial distance ($0 < r/a < 1$). Fink previously estimated solvent composition of a BCP photonic gel at given times (12 and 62 h after casting) along radial direction using time-dependent Fick's diffusion law assuming $c(r = a, t) = 0$ and $c(r, 0) = c_0$, where c is solvent concentration at a specific distance a and time t and c_0 is an initial concentration.[19] The concentration profiles derived in our experimental data (Figure 4b) follow the calculated profile in Fink's calculation quite well. Therefore, the polymer composition dependence of the lamellar domain spacings and the respective refractive indices account for the observed changes in reflective color from the self-assembled block copolymer gel.

Deviation from Modeled Calculation. Table 1 shows that the reflection of λ_{peak} at about 680 nm corresponds to a polymer concentration of approximately 65% and the lamellar period of 221 nm. Although our model calculation explains the tendencies for the increase of reflectivity peak intensity and peak broadening of each stop band fairly well, the calculated fwhm of each peak is strongly underestimated in comparison to the measured values, particularly in the higher polymer concentration regime. As noted before, for the TMM calculation, we assumed parallel lamellar layers throughout solvent evaporation. In our previous report, we observed the disruption of lamellar orientation at the edge of the sample during solvent evaporation using LSCM.[16] To investigate lamellar orientation in the solvent-swollen samples, plane-view images were taken along the radial direction using reflection mode LSCM. In reflection mode, image contrast relies on the change in refractive index between microdomains and grain boundaries. In Figure 5, each image shows the set of lamellar grains at the middle depth of the sample. It is obvious that there is a decrease in the average lamellar grain size as well as greater misorientations as the concentration of solvent decreases. Disruption of the lamellar grains can be attributed to the drying stresses occurring during solvent evaporation.

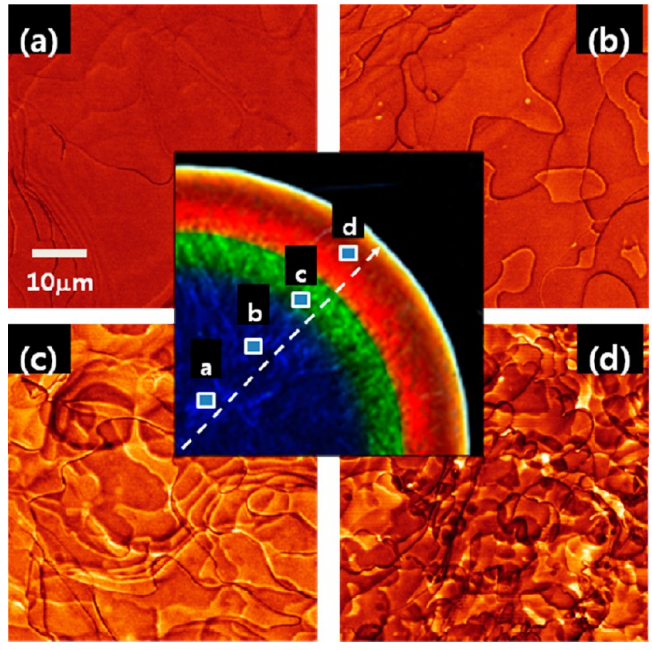

Figure 5. Planar (XY) LSCM images taken at the midplane thickness at different radial positions. The locations from which each LSCM image was taken are indicated in the photograph shown at the center. The sample corresponds to 14 h postcasting. As evident, drying forces cause considerable wrinkling and disruption of the lamellae.

By taking a time series of LSCM images, we noted that the radial diffusion of solvent actually causes movement and distortion of the lamellar grains, resulting in radial polymer

dx.doi.org/10.1021/ma302557v | Macromolecules 2013, 46, 6528–6532

mass flow during solvent evaporation. As indicated in our previous investigation, global movement of lamellar grains is induced by shear stress particularly for the BCP gel near the substrate.[16] This shear force likely causes the disruption of the lamellar orientation resulting in the significantly broader fwhm of the peak reflectivity due to the angular dependence of the reflectivity and diffuse scattering from the polygranular textures.

■ CONCLUSIONS

In summary, the dynamic structural color change of a high molecular weight lamellar PS-*b*-PI BCP gel was studied during isothermal solvent evaporation using reflectivity and confocal microscopy. The dependence of the lamellar period and hence the peak reflectivity on solvent concentration (via the effective Flory–Huggins interaction parameter) leads to a strong red-shift with increasing polymer concentration. Because of the high molecular weight of the BCP employed, ($\sim 10^6$ g/mol) microphase separation initially occurs at a polymer concentration as low as 10% and thus, during evaporation, the peak intensities from the lamellar microphases cover the whole visible spectrum at different radial positions. The experimentally observed reflectivity along the radial direction was compared to TMM simulations in order to extract the radial dependence of the solvent concentration. The time evolution of the concentration profile was in reasonable agreement with a previous theoretical calculation.[19] Confocal microscopy showed direct evidence of the disruption of the parallel lamellar morphology during solvent evaporation, accounting for the observed broadening of the reflectivity peak due to the tilted lamellar layers and scattering from the polygranular textures.

■ AUTHOR INFORMATION

Corresponding Author

*E-mail: elt@rice.edu (E.L.T.); hyunjung@kookmin.ac.kr (H.L.).

Author Contributions

[⊥]W.L. and J.Y. contributed equally to this work.

Notes

The authors declare no competing financial interest.

■ ACKNOWLEDGMENTS

This research was supported by the U.S. Army Research Office (USARO) through the Institute for Soldier Nanotechnologies, under contract W911NF-07-D-0004, and a Division of Materials Research Polymer Program NSF grant DMR-0804449. H. Lee acknowledges the financial support of this work by the National Research Foundation of Korea Grant funded by the Korean Government (MEST) (NRF-2009-C1AAA001-0093049 and 2012R1A2A2A01014288). W. Lee acknowledges the financial support by the National Research Foundation of Korea (NRF) grant funded by the Korea government (MSIP) (No. 2008-0061892). J. Yoon gratefully acknowledges support from the U.S. National Science Foundation under Award No. ECCS-1202522. The set of images in Figure 1 was kindly supplied by Ms. Felice Frankel.

■ REFERENCES

(1) Park, C.; Yoon, J.; Thomas, E. L. *Polymer* **2003**, *44* (22), 6725–6760.
(2) Lodge, T. P. *Macromol. Chem. Phys.* **2003**, *204* (2), 265–273.
(3) Lee, C.; Kim, S. H.; Russell, T. P. *Macromol. Rapid Commun.* **2009**, *30* (19), 1674–1678.
(4) Haberkorn, N.; Lechmann, M. C.; Sohn, B. H.; Char, K.; Gutmann, J. S.; Theato, P. *Macromol. Rapid Commun.* **2009**, *30* (14), 1146–1166.
(5) Kang, Y.; Walish, J. J.; Gorishnyy, T.; Thomas, E. L. *Nat. Mater.* **2007**, *6* (12), 957–960.
(6) Joannopoulos, J. D.; Meade, R. D.; Winn, J. N. *Photonic Crystals: Molding the Flow of Light*; Princeton University Press: Princeton, 1995.
(7) Deng, T.; Chen, C. T.; Honeker, C.; Thomas, E. L. *Polymer* **2003**, *44* (21), 6549–6553.
(8) Urbas, A. M.; Thomas, E. L.; Kriegs, H.; Fytas, G.; Penciu, R. S.; Economou, L. N. *Phys. Rev. Lett.* **2003**, *90* (10), 108302.
(9) Yoon, J.; Mathers, R. T.; Coates, G. W.; Thomas, E. L. *Macromolecules* **2006**, *39*, 1913–1919.
(10) Yoon, J.; Lee, W.; Thomas, E. L. *Nano Lett.* **2006**, *6* (10), 2211–2214.
(11) Yoon, J.; Lee, W.; Thomas, E. L. *Macromolecules* **2008**, *41*, 4582–4584.
(12) Edrington, A. C.; Urbas, A. M.; DeRege, P.; Chen, C. X.; Swager, T. M.; Hadjichristidis, N.; Xenidou, M.; Fetters, L. J.; Joannopoulos, J. D.; Fink, Y.; Thomas, E. L. *Adv. Mater.* **2001**, *13* (6), 421–425.
(13) Leiblert, L. *Macromolecules* **1980**, *13*, 1602–1617.
(14) Chan, E. P.; Walish, J. J.; Thomas, E. L.; Stafford, C. M. *Adv. Mater.* **2011**, *23* (40), 4702.
(15) Chan, E. P.; Walish, J. J.; Urbas, A. M.; Thomas, E. L. *Adv. Mater.* **2013**, *25*, 3934–3947.
(16) Lee, W.; Yoon, J.; Lee, H.; Thomas, E. L. *Macromolecules* **2007**, *40*, 6021–6024.
(17) Balsara, N. P.; Eastman, C. E.; Foster, M. D.; Lodge, T. P.; Tirrell, M. *Makromol. Chem., Macromol. Symp.* **1991**, *45*, 213–235.
(18) Maldovan, M.; Thomas, E. L. *Periodic Materials and Interference Lithography: For Photonics, Phononics and Mechanics*; Wiley-VCH Publishers: Weinheim, 2009.
(19) Fink, Y. Block Copolymer Photonic Crystal. PhD Thesis in Materials Science at MIT, Cambridge, 2000.